



## Nanoscale Layers in Polymers to Promote Ion Transport

Journal:	<i>Molecular Systems Design &amp; Engineering</i>
Manuscript ID	ME-PER-11-2018-000086.R1
Article Type:	Perspective
Date Submitted by the Author:	08-Jan-2019
Complete List of Authors:	Trigg, Edward; University of Pennsylvania, Materials Science & Eng. Winey, Karen; University of Pennsylvania, Materials Science and Engineering

SCHOLARONE™  
Manuscripts

### Design, System, Application Statement

In this perspective, we discuss the design of polymers to achieve layered nanostructures advantageous for charge transport. Recent studies have revealed that precisely periodic placement of functional groups along a linear methylene backbone can lead to hairpin chain folding at the position of each functional group when the polymer crystallizes. This, in turn, produces well-controlled layers of the functional groups. This layered structure is robust across a wide array of groups that include acids, ions, and oligomeric side chains immiscible with the methylene backbone. There is a large design space within this paradigm to engineer layered structures with desired properties, by adjusting the functional group chemistry and periodicity as well as the backbone chemistry.

# Nanoscale Layers in Polymers to Promote Ion Transport

Edward B. Trigg<sup>†</sup> and Karen I. Winey\*

Department of Materials Science and Engineering, University of Pennsylvania, Philadelphia PA 19104,  
United States

<sup>†</sup>Present Address: Air Force Research Laboratory RXCC, Wright-Patterson Air Force Base, Dayton, Ohio  
45433-7750, United States

\*Email: [winey@seas.upenn.edu](mailto:winey@seas.upenn.edu)

**Abstract**

Polymer membranes with enhanced charge transport properties would enable solid-state batteries with improved safety, increased lifetime, and decreased cost. However, the ion conductivity of polymers remains low after decades of research. Here, we advocate for an alternative design strategy for ion-conducting polymers, wherein a precisely periodic chemical microstructure leads to backbone crystallization, controlled hairpin chain folding at the position of each functional group, and ordered layers of sub-nanometer thickness that function as pathways for charge transport. This chain-folded layered structure is observed in a linear polyethylene with sulfonic acid groups pendant to precisely every 21<sup>st</sup> carbon atom, and the membrane exhibits high proton conductivity at high humidity, matching the benchmark membrane Nafion 117. We discuss related instances of ion and proton transport through thin layers in polymers, as well as other examples of controlled polymer folding leading to ordered nanoscale layers. We also propose design rules for achieving the chain-folded layered structure in new polymers. This layered structure has the potential for improved charge transport relative to amorphous polymers, representing a significant advance in ion-conducting polymer membranes.

## 1. Introduction

The development of low-cost, high-performance solid state batteries would have enormous societal benefits, including improved safety and efficiency for electric vehicles and increased viability for intermittent renewable energy sources such as solar and wind. To enable this, the liquid electrolytes found in traditional batteries would need to be replaced by solid electrolytes with high ion conductivity, near-zero electron conductivity, high mechanical integrity, and the ability to form ion-transferring interfaces with the electrodes. Various polymer systems are often proposed for this application, including polymer-salt complexes, gel polymers, and single ion conducting polymers.<sup>1</sup> The latter contain only one mobile ion species, e.g., lithium, and thereby prevent polarization of the anions during battery operation, another benefit. A lack of viable polymer electrolyte materials has prevented commercialization of solid state batteries. In particular, the ion conductivity of solid polymers needs to be increased.

Traditionally, ion-conducting polymeric membranes rely upon amorphous polymer for ion transport. A typical example is poly(ethylene oxide) (PEO) (either at  $T > T_m$  or crosslinked to suppress crystallization) with a dissolved salt such as lithium bis(trifluoromethanesulfonyl)imide (LiTFSI). The ether oxygens in the PEO associate with lithium ions, enabling charge separation. The resulting ion conductivity scales with the polymer's segmental dynamics (or structural relaxation). Because PEO is too soft to provide adequate mechanical separation between the electrodes, block copolymers such as poly(styrene-*b*-ethylene oxide) (PS-PEO) are often used.<sup>2</sup> With similar block molecular weights, these block copolymers exhibit lamellar microphase separation, and the PEO-salt domains provide lithium ion conductivity while the polystyrene (PS) domains provide mechanical rigidity. Although these contain conductive lamellar domains  $\sim 10$  nm thick, the ion conductivity mechanisms in these systems do not differ qualitatively from the PEO homopolymer.

In addition to polymers, some crystalline ceramic materials are also candidates for solid electrolytes.<sup>3</sup> While polymers possess many benefits over ceramics including good contact with the electrodes, high toughness, and processability, most polymers have insufficient conductivity. The highest known solid state lithium ion conductivity is found not in polymers but in ceramics, which are typically

single ion conductors. In fact, several crystalline ceramic materials exhibit lithium ion conductivities two orders of magnitude higher than the highest-performing polymers.<sup>4,5</sup> Since the discovery that ion conductivity occurs primarily in the amorphous phase of PEO,<sup>6</sup> researchers have often disregarded polymers with crystal-like ordering, focusing instead on amorphous polymers, and improvements in conductivity have been incremental. Here we make the case that specially-designed crystalline polymers could achieve conductivities approaching or surpassing those of the high-performing crystalline ceramics and advocate for additional research along this direction.

## 2. Ion and Proton Conductivity in Nanoscale Layers in Polymers

**Precise sulfonic acid polyethylene.** Recently, it was found that a linear polyethylene with precisely spaced pendant sulfonic acid groups<sup>7</sup> (termed “p21SA”) exhibits a layered structure with high proton conductivity when hydrated.<sup>8</sup> The polymer chains executed hairpin folds at the position of each sulfonic acid group, such that the alkyl segments crystallize and the acid groups assemble into layers (Figure 1a). Upon exposure to humid air, water molecules enter the hygroscopic sulfonic acid layers causing a reversible increase in layer period as seen via X-ray scattering. As the water content increases progressively with relative humidity (RH), the proton conductivity also increases. At RH of 60% or greater, the conductivity of p21SA is on par with Nafion 117 (Figure 1b), a benchmark proton conducting membrane. Both polymers reach conductivities of  $10^{-1}$  S/cm at 95% RH.

Atomistic molecular dynamics (a-MD) simulations were performed at a range of hydration levels to confirm and further investigate the structure and dynamics of p21SA. The layer periods from the simulations match those from experimental X-ray scattering at the same hydration number to within 1 Å. (The hydration number is the number of water molecules per sulfonic group.) This confirms the hairpin layer structure. The simulations showed that the thickness of the water layer sandwiched between the sulfonic groups approaches 10 Å at high RH. The proton conductivity occurs within these water layers and depends on a complex interplay between the percent acid dissociation, the hydrated proton concentration and distribution, the degree of confinement of water, the ordering and mobility of the acid

groups, and other factors. Water diffusion coefficients were quantified in the simulations and compared with amorphous structures of the same polymer at the same hydration levels. Water diffused several times faster in the crystalline simulations due to lower tortuosity and fewer bottlenecks in the hydrated layers, suggesting that the crystalline structure improves transport compared with the amorphous structure. This work demonstrates that a polymer with crystal-like ordering can give rise to efficient proton transport within highly confined hydrated layers.

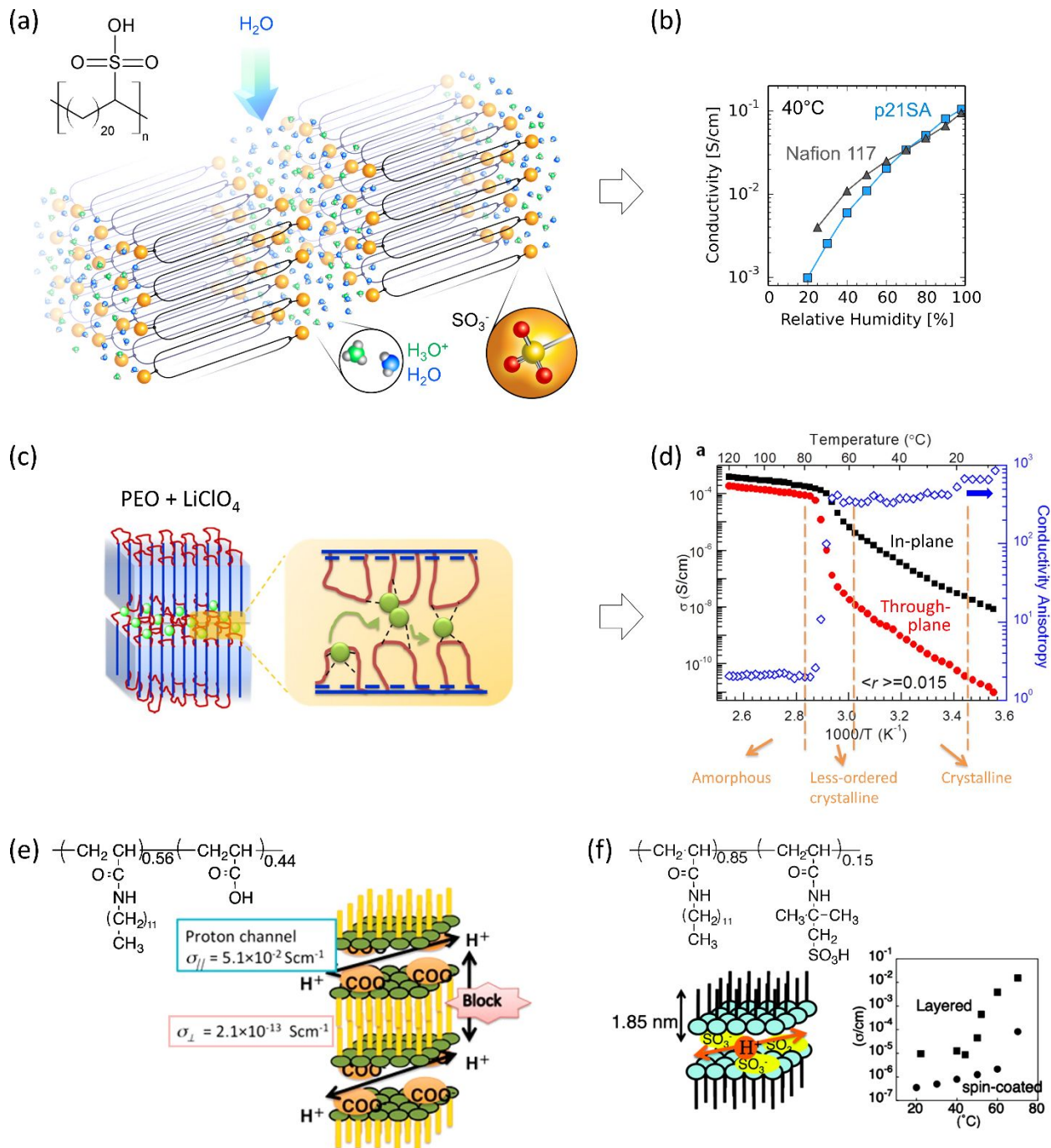


**Figure 1.** Chemical structures, morphologies, and conductivities of polymers that form 2D conductive layers. (a) A precisely sequenced sulfonic acid polyethylene forms a layered structure with controlled hairpin folding, leading to (b) proton conductivity on par with Nafion 117. Adapted from Trigg *et al.*<sup>8</sup> (c) Films of solution-grown single crystals of PEO are subsequently infused with  $\text{LiClO}_4$ , giving rise to (d) highly anisotropic ion conductivity. Adapted with permission from Cheng *et al.*<sup>9</sup> Copyright 2014

American Chemical Society. (e), (f) Random acid-containing copolymers forming layered structures with high proton conductivity. Adapted with permission from Sato *et al.*<sup>10</sup> and Matsui *et al.*<sup>11</sup> Copyright 2015 and 2011, American Chemical Society.

**PEO single crystal films.** Semicrystallinity is often believed to impede ion conductivity in polymer electrolytes, not only because the crystalline domains act as barriers to ion transport, but also because the amorphous polymer segments are tethered to crystalline segments, reducing segmental dynamics. To investigate the relationship between crystallinity and conductivity in PEO-salt complexes, Cheng *et al.* produced films of solution-grown single crystals of PEO (Figure 1c).<sup>9</sup> The single-crystal lamellae (~10 nm thick) were oriented in the plane of the films, and the films were 10-20  $\mu\text{m}$  thick, corresponding to  $\sim 10^3$  crystals in thickness. Lithium salt was added to these films by soaking them in  $\text{LiClO}_4$  pentyl acetate solution, followed by drying.

At low to moderate salt concentrations, the salt ions resided near the surfaces of the crystals, near the chain folds. These two-dimensional surface regions were 2-3 nm thick, several times thicker than the hydrated layers in p21SA. The conductivity of the films was highly anisotropic,<sup>12</sup> with the in-plane conductivity up to 2000x higher than the through-plane, indicating that the crystals do indeed block or significantly impede ion transport (Figure 1d). Interestingly, at moderate salt concentrations, the dynamics in the crystal surface regions are not significantly slowed by chain tethering, and the mobility is comparable to that of crosslinked PEO-salt complexes, which are fully amorphous at the same temperature. These findings support the idea that efficient ion transport can occur through thin, two-dimensional layers bordered by hairpin-folded, crystalline polymer.

**Proton-conducting polymer thin films.** Recent work by Matsui and coworkers has shown high proton conductivity in polymer thin films that form layered structures.<sup>10,11,13,14</sup> These polymers are not precisely sequenced and the layers do not consist of hairpin folding of polymer backbones. Instead, they are random copolymers composed of two monomers: one with a long, hydrophobic side chain, and the other with a short, acid- or amine-terminated side chain (Figures 1e, 1f). By casting on a water surface

from chloroform solution,<sup>11</sup> a stable nanosheet forms wherein hydrated sulfonic acid groups form highly ordered layers in the plane of the film, as observed via X-ray diffraction. With various chemistries and processing techniques, these thin films showed high conductivities, in the range of  $10^{-2} - 10^{-1}$  S/cm.

### 3. Controlled Hairpin Folding in Polymers

Considering the high conductivity of the controlled hairpin-folding polymer p21SA, here we review polymers with similar hairpin-folding structures. The many examples in the literature show that there is ample opportunity to design new hairpin-folding polymers for electrolyte applications. Note that block copolymers that form microphase separated lamellar morphologies do not possess hairpin folds and thus are excluded from this discussion.

**Precise ionenes.** The link between precisely periodic placement of interacting functional groups along a polymer backbone and control over chain folding was first proposed decades ago. Aliphatic ionenes (polymers with charged groups in the backbone) with precisely periodic dimethylammonium groups were originally produced in 1968.<sup>15</sup> In the early 1980s, Kunitake *et al.* observed that these precise ionenes form vesicles in water.<sup>16,17</sup> The vesicle walls were composed of chain-folded ionenes that gave rise to lipid bilayer like structures (Figure 2b). The authors also synthesized small-molecule analogues to the ionenes, consisting of one ionic group and two alkyl chains (similar to Figure 2a) or two ionic groups and three alkyl chains. Like the ionenes, these also fold at the positions of the ionic groups to form bilayers. In the polymers and the small molecules, a minimum alkyl chain length is required for the layer structure to occur: with at least 18 methylene units, the layers form, but with 16 or fewer they generally do not. Presumably, the hydrophobic interactions between alkyl segments must reach a critical point to overcome the entropic and conformational free energy penalties of forming the layers. Another ionene was produced that was a random copolymer containing both  $C_{20}$  and  $C_{16}$  methylene segment lengths, and this did not form layers.<sup>17</sup> The effect of imprecision in polymer microstructure on layer formation will be discussed later in this article.

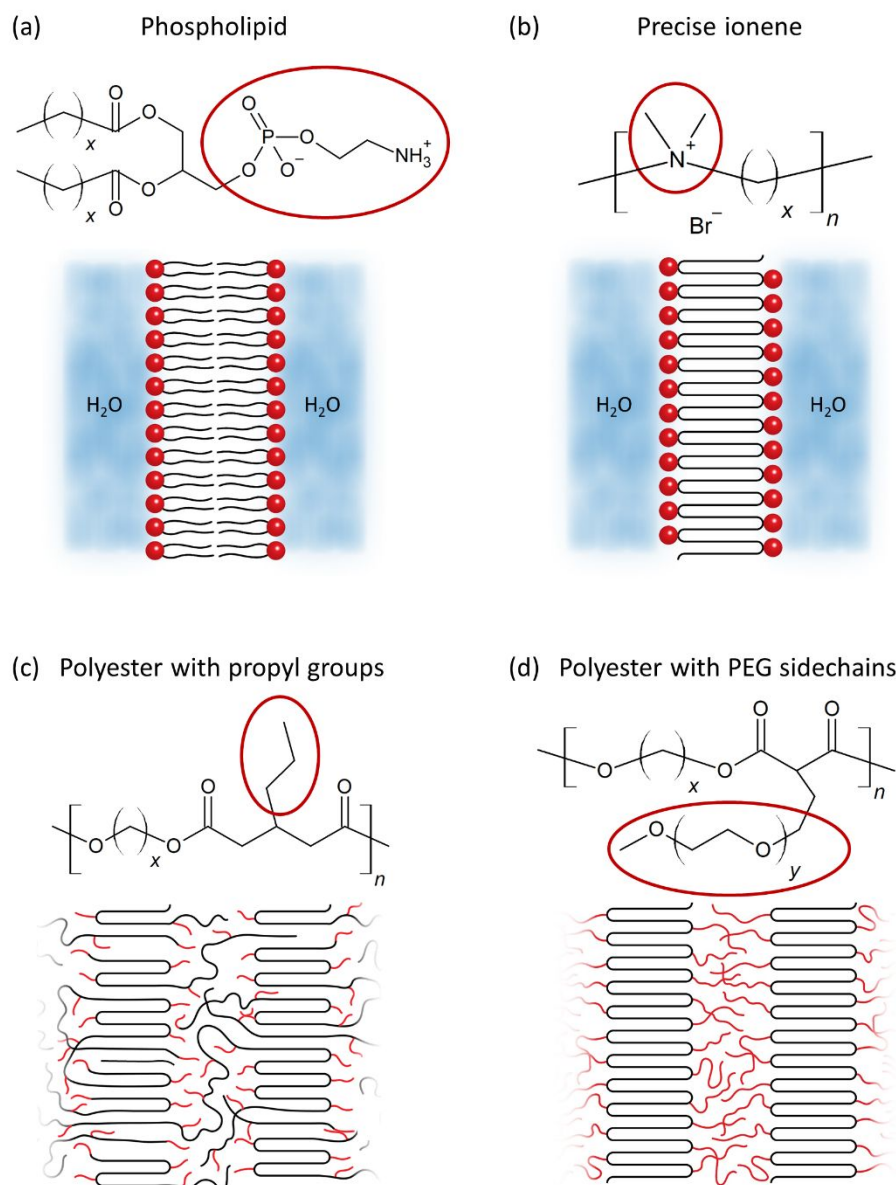


**Figure 2.** (a) Classical lipid bilayer (phosphatidylethanolamine), and (b) a precise ionene folding to form a similar structure in water, drawn based on results from Kunitake *et al.*<sup>16</sup> (c) Chain folding in an aliphatic polyester is controlled by precisely spaced propyl side groups, drawn based on results from de Ten Hove *et al.*<sup>18</sup> (d) Chain folding in another aliphatic polyester is controlled by oligomeric PEG side chains, drawn based on results from Chanda *et al.*<sup>19</sup> The functional groups that induce folding are circled in red and represented by the red circles or lines.

The effect of chemically modifying the hydrophobic segments on layer formation was also investigated. Two more ionenes were made where, at the center of each methylene segment, one and two phenol groups were incorporated into the backbone.<sup>17</sup> Interestingly, the authors concluded that incorporation of one or two phenol units did not prevent formation of the chain-folded layers, and actually increased the melting temperature ( $T_m$ ) of the layered structures from 53°C to 63°C and 62°C, respectively (see Figure 4), as seen via differential scanning calorimetry (DSC). In 2000, Hong *et al.* found that a similar incorporation of oxyazobenzyl groups into the ionene backbones still permitted the ordered, chain-folded layered structures to form.<sup>20</sup> In Hong's case, the layers were observed in thin films produced via layer-by-layer electrostatic deposition.

A recurring issue with these ionenes is the difficulty in directly detecting the chain-folded layered structure. The evidence presented by Kunitake consists of (i) vesicles and/or disks observed via TEM after staining with uranyl acetate, where the vesicle wall or disk thickness was comparable to the all-*trans* length of the repeating unit, and (ii) a sharp endothermic transition within the expected temperature range via DSC. Hong *et al.* presented spectroscopic evidence of backbone ordering as well as atomic force microscopy (AFM) data showing regular steps in height. While the evidence is convincing, these studies also demonstrate the inherent difficulty of unambiguously showing the presence of hairpin folding in an imperfectly ordered polymer.

**Precise polymers with short side chains.** An alternative route to inducing a hairpin fold is to introduce a short side chain that is incompatible with the crystalline structure of the polymer backbone. De Ten Hove and coworkers synthesized polymers with precisely spaced alkyl groups (Figure 2c) that exhibit controlled chain folding when crystallized from the melt.<sup>18</sup> These polyesters were synthesized from long aliphatic diols ( $C_{22}$  or  $C_{44}$ ) and glutaric acid or 3-*n*-propylglutaryl dichloride, and the latter incorporates a propyl side group near the ester groups along the chain. Without the propyl group, the polymers behave similarly to HDPE or a standard aliphatic polyester, forming the typical lamellar semi-crystalline morphologies. However, the addition of the propyl group dictates the lamellar thickness because it is too large to be incorporated into the crystal as a defect. This has been confirmed by Rojas *et*

*al.*<sup>21</sup> The crystalline lamella thickness (as measured by AFM, TEM, and SAXS) of the polymer made from C<sub>44</sub> diol and 3-*n*-propylglutaryl dichloride monomers was independent of crystallization temperature over a range of more than 60°C. Patterson function analysis of SAXS data revealed a higher electron density at the lamellar surfaces, indicating a high concentration of branch points (propyl groups). The authors conclude that a significant portion of the chains must form tight folds at the lamellar surfaces due to density considerations.

In addition to the copolymerization techniques that produced the precise polymers described above, precise polymers can be synthesized via acyclic diene metathesis (ADMET) polymerization.<sup>22</sup> With ADMET, symmetric diene monomers that contain functional groups at their centers are homopolymerized to yield linear polyethylene with precisely spaced functional groups.<sup>23</sup> Wagener's group has pioneered this versatile technique, producing polyethylenes with tens of different functional groups,<sup>24</sup> including alkyl,<sup>25</sup> halide,<sup>26</sup> acid,<sup>7,27,28</sup> and oxidized sulfur<sup>29,30</sup> functionalities. These functional groups are typically bonded to every 9<sup>th</sup>, 15<sup>th</sup>, or 21<sup>st</sup> carbon along the backbone.

ADMET polyethylenes were synthesized by Wagener's group containing short poly(ethylene glycol) (PEG) side chains on every 15<sup>th</sup> or 21<sup>st</sup> carbon.<sup>31,32</sup> For the methylene length of 20, DSC revealed two endothermic transitions upon heating, which were attributed to methylene crystallinity and PEG crystallinity. The PEG segments, four and five repeat units in length, were excluded from the methylene crystalline regions, as found by extensive DSC analysis. On this basis, tight chain folds were presumed to dominate the surfaces of the methylene crystals, with the PEG branch points at the folds.

Building on this initial work, Ramakrishnan's group produced aliphatic polyesters with precisely spaced short side chains composed of PEG<sup>19,33,34</sup> (Figure 2d) or poly(tetrafluoroethylene) (PTFE).<sup>35</sup> These polymers also form chain-folded layers from the melt state upon cooling. For the polyesters with side chains containing between 3 and 16 PEG units, SAXS on bulk samples revealed a layered structure with well-defined periodicity of order 5 nm, consistent with a chain folding motif.<sup>33</sup> This periodicity was tunable by changing the PEG length, and by random co-grafting with two PEG lengths.<sup>19</sup> In contrast with the polyesters containing propyl side chains, this morphology consists of *multilayers* of hairpin folding.

AFM was also performed on spin-coated and thermally annealed thin films, and structures were observed with well-defined step heights consistent with the SAXS periodicity.

For the PTFE-grafted polyesters, TEM was employed to observe the long-range ordering of the alternating methylene and PTFE layers.<sup>35</sup> Remarkably, the layers persist for hundreds of nanometers without significant changes in orientation, both laterally and along the layer normal. This suggests an absence of domains composed of amorphous (disordered) polymer backbones, in sharp contrast with classical semicrystalline polymers. By combining SAXS, AFM, and TEM, as well as DSC and FTIR spectroscopy, these studies provide ample convincing evidence for well-controlled chain folding in this family of polyesters.

**Precise polymers with polar pendant groups.** Intermediate between the ionenes with a charged group in the backbone that chain fold to satisfy coulombic interactions and the precise polymers with short side chains that chain fold primarily to maximize backbone crystallization are precise polymers with polar pendant groups. In this class of polymers, chain folding is driven by both secondary bonding between pendant groups and crystallization of the backbone. Over the last decade, acid-containing polymers and ionomers have been produced by ADMET polymerization. Linear polyethylenes with precisely periodic carboxylic acid,<sup>27</sup> phosphonic acid,<sup>28</sup> imidazolium bromide,<sup>36</sup> sulfonic acid,<sup>7</sup> and sodium sulfonate<sup>7</sup> were made by Wagener's group (see Figure 3a,b). Recently, our group investigated the structure of a polyethylene with carboxylic acid groups pendant to every 21<sup>st</sup> carbon (termed *p21AA*).<sup>37</sup> While layers are clearly evident in bulk crystallized p21AA via X-ray scattering, with small side groups the possibility of extended-chain layers must also be considered. Extended-chain layers refer to a crystal structure like those of nylons, where the chains are nearly all-trans and the functional groups form layers due to secondary bonding and/or steric effects.

Using atomistic molecular dynamics (a-MD) simulations, X-ray scattering, and Raman spectroscopy, it was found that hairpin chain folding takes place at the position of each acid group, giving rise to multiple consecutive layers of folded polymer (Figure 3c). The presence of multiple consecutive layers is related to the PEG-grafted polyesters (Figure 2d); however, it differs in important ways. The side

group interactions are quite distinct: in the PEG-grafted polyesters, the long, flexible PEG side groups ( $M_w = 252$  Da)<sup>33</sup> will have significantly different enthalpic and entropic interactions compared with single carboxylic acid groups ( $M_w = 45$  Da). Also, p21AA contains amorphous domains as well as crystalline, chain-folded domains, and these two phases exist in alternating layers or lamellae. Interestingly, the acid layer planes are approximately perpendicular to the crystalline-amorphous layer planes (Figure 3d).<sup>38</sup> This structure has not been reported in any other hairpin folding polymers to date.

Using different crystallization methods, Ortmann *et al.* found that p21AA can also form structures resembling the precise ionenes of Kunitake *et al.*<sup>39</sup> They prepared single crystals of p21AA from a dilute tetrahydrofuran (THF) solution that also contained CsOH. Presumably, some of the carboxyl groups were neutralized with Cs<sup>+</sup>. TEM showed that these single crystals had a thickness of  $\approx 3$  nm, roughly corresponding to one all-trans repeat unit. The methylene segment length between carboxyl groups was increased to 45 and the single crystal thickness increased to  $\approx 6$  nm. This suggests that the single crystals consist of one layer of hairpin-folded chains with the crystal surfaces containing the carboxyl groups.

Chain-folded layers are also formed by polyethylene with imidazolium bromide groups pendant to every 21<sup>st</sup> or 15<sup>th</sup> carbon atom (termed *p21ImBr* and *p15ImBr*, respectively, Figure 3h). Single crystals of p21ImBr were grown from dimethyl sulfoxide (DMSO) solution, and abnormally large crystal thicknesses were observed: up to 850 nm. These crystals are more than an order of magnitude thicker than typical solution-grown crystals of polyethylene (Figure 3g).<sup>40</sup> These thick crystals contained at least 150 chain-folded layers, and the thickness was several times larger than the extended chain length, based on the molecular weight. This is in sharp contrast with Kunitake's ionenes, which also contained precisely periodic ionic groups but in water formed thin vesicles or disks consisting of only about 2 layers. This difference in assembly, although not yet sufficiently explored, could be related to polymer flexibility, thermal treatment, or choice of solvent.

The morphology of p21ImBr when crystallized from the melt appears to resemble the solution-grown crystals. X-ray scattering of bulk, melt-crystallized p21ImBr showed a layer periodicity of 33 Å.<sup>41</sup>

This is larger than the all-*trans* length of the repeating unit, demonstrating that these are hairpin layers, not extended chain layers. The layer peaks were very narrow, indicating well-ordered layers, and the large grain size of p21ImBr more closely resembles the PEG-grafted polyesters than p21AA.

Finally, when sulfonic acid groups are used in place of carboxyl or imidazolium bromide (p21SA, Figure 1a), there is ample evidence for chain-folded layers (Figure 3f).<sup>8</sup> When exposed to a humid environment, X-ray scattering shows expansion of the layer periodicity by more than 10%, well beyond the all-*trans* length of the repeating unit. This reversible expansion would not be possible with extended chain layers. Also, a-MD simulations of p21SA in the hairpin layer structure were performed at various hydration levels (Figure 3e), and the layer periodicity as a function of hydration matched experiments to within 1 Å. Similar to p21ImBr, and in contrast with p21AA, the grain size of the layers in p21SA was very large, at least 70 nm.

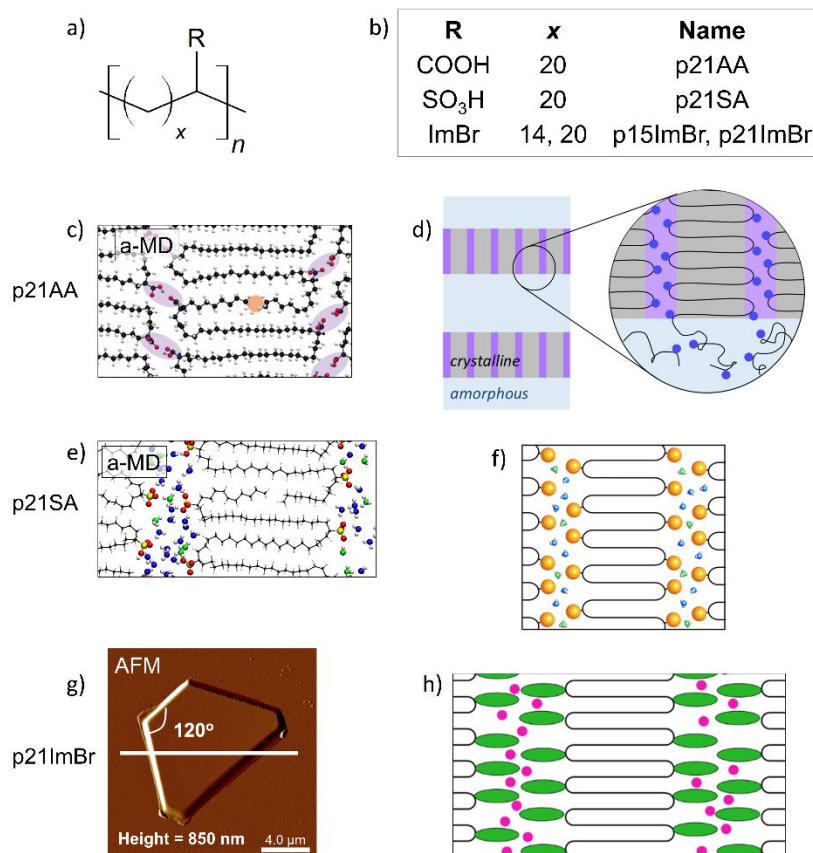


**Figure 3.** (a) General structure of acid- and ion-containing ADMET polyethylenes, and (b) specific ADMET polyethylenes discussed in this work. (c) A 2D slice of a snapshot from an atomistic molecular dynamics simulation of p21AA,<sup>37</sup> and (d) a schematic of the (idealized) semicrystalline structure of that polymer.<sup>38</sup> (e) A 2D slice of a snapshot from an atomistic molecular dynamics simulation of hydrated p21SA, and (f) a schematic of its crystalline structure.<sup>8</sup> (g) Atomic force microscope image of a solution-grown single crystal of p21ImBr,<sup>40</sup> and (h) a schematic of its crystalline structure.<sup>42</sup> Adapted with permission from (c) Trigg *et al.*,<sup>43</sup> (d) Trigg *et al.*,<sup>38</sup> (e)-(f) Trigg *et al.*,<sup>8</sup> (g) Yan *et al.*,<sup>40</sup> and (h) Trigg *et al.*<sup>42</sup> Copyright 2017 American Chemical Society, 2017 American Chemical Society, 2018 Nature Publishing Group, 2017 Elsevier, and 2018 American Chemical Society.

Figure 4 shows the melting temperatures ( $T_m$ ) of various hairpin layer forming polymers, as well as *n*-alkanes and phospholipids (sketched in Figure 2a) for comparison.  $T_m$  is plotted as a function of the

number of methylene units per repeating unit ( $n_{\text{CH}_2}$ ). With the exception of the imidazolium bromide polymers, all the hairpin folding polymers have  $T_m$ s relatively close to the alkane with the same number of methylene units. Polymers containing associating groups such as ions or strongly hydrogen-bonding acids tend to have higher  $T_m$ s than those with alkyl or PEG side groups. Given the same  $n_{\text{CH}_2}$ , phospholipids have higher  $T_m$ s than any of the polymers expect for those containing imidazolium bromide. The high melting points of the imidazolium bromide polyethylenes (open green triangles in Figure 4) might be explained by the geometry of the functional group: (i) the size and shape of the functional group allows for efficient packing, and (ii) the extra methylene unit linking the imidazolium group to the backbone provides added flexibility to improve packing.

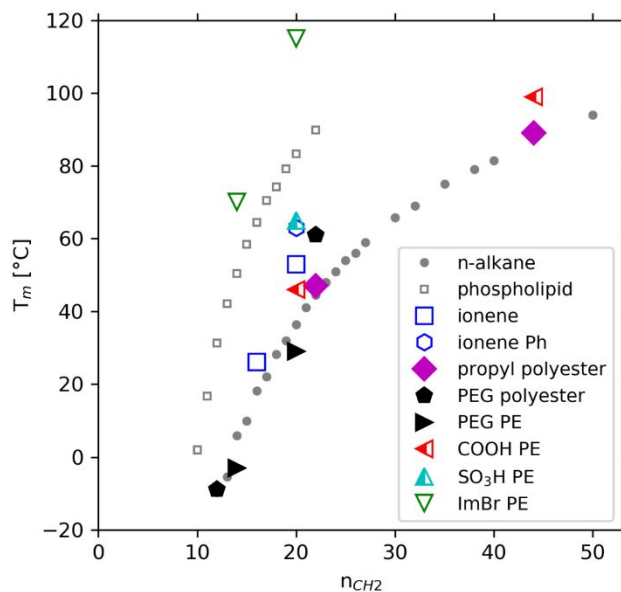


**Figure 4.** Melting temperatures of various hairpin layer forming polymers and some small molecules for comparison, as a function of the number of backbone methylene units per repeating unit. Plotted are selected *n*-alkanes of lengths 9 to 50;<sup>44</sup> the phospholipid family phosphatidylethanolamine, having two identical saturated alkyl tails, which forms lipid bilayer membranes;<sup>45,46</sup> dimethylammonium ionenes with and without phenol (Ph) groups;<sup>17</sup> polyesters with propyl side groups;<sup>18</sup> polyesters with PEG side groups;<sup>33</sup> and ADMET polyethylenes with PEG side groups,<sup>31</sup> carboxylic acid pendant groups,<sup>27,39</sup> sulfonic acid pendant groups,<sup>7,8</sup> and imidazolium bromide pendant groups.<sup>36,47</sup> Open symbols are ion-containing materials, half-filled symbols are acid-containing, and filled symbols contain neither ions nor acids. Triangles are ADMET functionalized polyethylenes. For the phospholipids,  $n_{CH_2}$  corresponds to the length of *each* tail.

#### 4. Alternative Strategies for Achieving Ordered Nanoscale Layers

**Telechelic association.** Hairpin folding of precise polymers is not the only way to achieve functional group layers with crystal-like order. Ordered layers can also be produced by end-functionalizing crystallizable polymers or oligomers with strongly associating groups. German *et al.* functionalized polyethylene chains ( $M_n = 1.3$  and 2.2 kDa) with thymine (Thy) or 2,6-diaminotriazine

(DAT) groups.<sup>48</sup> The Thy and DAT groups associate with one another with three hydrogen bonds, providing strong but temporary linkages. When cooled from the melt, these short telechelic polymers self-assembled into layers upon crystallization, with a layer period between 91 and 200 Å depending on  $M_n$  and other factors. More recent work by the same group reported layers with very long range order, achieved via thermal treatment,<sup>49</sup> and extended the concept to PEO chains.<sup>50</sup> Given an appropriate choice of functional group, these telechelic associators may be useful for proton or ion transport.

## 5. Design Rules for Controlled Chain Folding

Given the promise of controlled chain folding for enhanced charge transport in polymer systems, we present here a list of conjectural design rules for achieving the layered, chain-folded structures, based on available data.

**Backbone segment length.** Using crystallizable backbone segments appears to be a good strategy for achieving chain-folded layers, because the driving force for crystallization compels the chains to fold. Methylene segments have primarily been used to date, due to chemical stability and synthetic versatility, but other crystallizable backbones such as PEO or PTFE may also give rise to the layers. Regardless, the backbone segments must be sufficiently long ( $x$  sufficiently large in Figure 5) that the crystallization temperature is greater than the  $T_g$  of the polymer; otherwise, the layered structure will not be accessible. The observed melting temperature in the layer-forming polymers with methylene backbones is usually equal to or slightly greater than that of an alkane with the same number of methylene segments (Figure 4). Based on the available data, a minimum of 15-20 methylene units is typically sufficient for layer formation. The minimum length depends upon the choice of functional group.

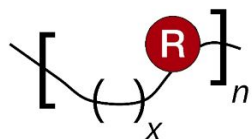


**Figure 5.** A linear polymer with  $R$  groups at intervals of  $x$  along the backbone. The main factors affecting whether the polymer will form the hairpin layer structure are as follows: backbone chemistry, length of  $x$ , uniformity of  $x$ , size of  $R$ , and miscibility between  $R$  and the backbone.

**Microstructure precision.** One would expect that polymers with randomly placed functional groups (i.e., random  $x$  in Figure 5) will not form the hairpin layer structure. Indeed, this has been found experimentally: Baughman *et al.* produced polyethylene with pseudo-randomly placed carboxylic acid groups as a comparison with the precise version, and no layers were visible in the X-ray scattering patterns.<sup>27</sup> Likewise, Kunitake *et al.* copolymerized the monomers from the  $C_{20}$  and  $C_{16}$  precise ionenes ( $x$  either 16 or 20), and this copolymer formed no structures from solution.<sup>17</sup> However, it is not yet known whether *small* deviations in  $x$  (Figure 5) will prevent the layered structure from forming. These nearly precise polymers might be more straightforward to synthesize and thus more commercially feasible. Recently, a polyester was synthesized that contained carboxylic acid groups with nearly precise periodicity along the chain;  $x$  was either 11 or 12.<sup>51</sup> No layers formed because  $x$  was too small. However, the X-ray scattering peaks of the amorphous polymer bore a strong resemblance to truly precise amorphous polymers, in both their positions and widths. This resemblance persisted in the ionomer forms, after neutralization with sodium. These results necessitate the synthesis of nearly precise polymers with larger  $x$ , to see if the chain-folded layers can be achieved.

**Functional group size.** The size of the functional group  $R$  (Figure 5) plays an important role in the hairpin layer-forming ability of the polymer. On the one hand, a very small  $R$  group can be incorporated into a polyethylene-like crystal structure, such as amide groups (nylons), methyl groups,<sup>25,52</sup> halide groups,<sup>26,53</sup> and sulfone groups.<sup>29</sup> The resulting structures resemble classical semicrystalline polyethylene, not hairpin layers. On the other hand, consider a rigid, bulky  $R$  group with a cross-sectional

area much greater than two crystalline alkyl segments. (The cross-sectional area of two crystalline alkyl segments is roughly equal to the a-b area of the orthorhombic polyethylene unit cell,  $36 \text{ \AA}^2$ .) For the hairpin layers to form, steric constraints would require a very large tilt angle between the crystalline stems and the functional group layers, and this may prevent layer formation altogether. An example of this is an ADMET polyethylene where  $R = (\text{PO}_3\text{H}_2)_2$  and  $x = 20$ . Ordinarily, the 20 methylene units should be sufficient for layer formation, but instead this polymer is amorphous with phosphonic acid clusters occupying a face-centered cubic lattice.<sup>54</sup> The two phosphonic groups have a large molecular volume of approximately  $100 \text{ \AA}^3$ ,<sup>55</sup> and furthermore the rigidity of the groups frustrate packing, preventing layer formation.

**Functional group miscibility.** The available data to date suggests that the multilayer hairpin layer structure forms when the functional group has low miscibility with the backbone. With methylene backbones, consecutive layers form when the  $R$  group is PEG, PTFE, carboxylic acid, dimethylammonium, etc., but not when the  $R$  group is an alkyl group. This may be related to the melt-state morphology, where less miscible groups would be expected to associate or aggregate, while alkyl groups may not. More research is required to fully understand the relationship between backbone- $R$  group miscibility and consecutive layer formation.

**Using peptide-inspired structures.** It may be possible to encourage controlled hairpin chain folding for a wider range of side groups or backbone structures. Under particular conditions, peptides such as MAX1 reliably execute a single fold with a defined set of molecular conformations, known as  $\beta$ -hairpin folding.<sup>56,57</sup> MAX1 contains two backbone pyrrolidine rings, each bonded to the backbone at positions 1 and 2. By incorporating cyclic groups into a polymer backbone in this way, this peptide-inspired strategy could be adapted to boost the chain folding proclivity of precise or nearly precise polymers.

## 6. Conclusion

In the development of new electrolytes for solid state devices, self-assembled nanoscale layers may prove a useful strategy for increasing proton or ion conductivity without sacrificing mechanical stability. In this Perspective, we have discussed many examples of polymers with precisely spaced functional groups that execute hairpin folds at the position of each functional group to produce nanoscale layers. These hairpin layers appear to be a robust and reliable consequence of precise sequencing, with certain constraints laid out in Section 5. We have also shown several examples of high conductivity in polymers with layers. This work beckons the synthesis of new precisely (or nearly precisely) sequenced polymers with functional groups specially designed for charge transport, e.g., LiTFSI groups. Such polymers will most likely form hairpin layer structures and may give rise to transport mechanisms that are distinct from those found in amorphous polymers, which dominate the literature to date. Considering the high lithium ion conductivity found in some crystalline ceramic materials, this strategy may lead to polymers with sufficient ion conductivity to enable the widespread commercialization of solid state batteries.

## Author Information

Corresponding Author

\*Email: [winey@seas.upenn.edu](mailto:winey@seas.upenn.edu) (K.I.W.)

ORCID

Edward B. Trigg: 0000-0002-4723-650X

Karen I. Winey: 0000-0001-5856-3410

Present Address

E.B.T.: Air Force Research Laboratory RXCC, Wright-Patterson Air Force Base, Dayton, Ohio  
45433-7750, United States

The authors declare no competing financial interest.

## Acknowledgements

The authors acknowledge funding from the National Science Foundation (NSF) DMR 1506726 and NSF PIRE 1545884. We acknowledge Charles Lee-Georgescu for illustrating Figures 1a and 2 as well as the table of contents figure.

## Conflict of Interest

There are no conflicts of interest to declare.

## References

- (1) Zhang, H.; Li, C.; Piszcz, M.; Coya, E.; Rojo, T.; Rodriguez-Martinez, L. M.; Armand, M.; Zhou, Z. Single Lithium-Ion Conducting Solid Polymer Electrolytes: Advances and Perspectives. *Chem. Soc. Rev.* **2017**, *46* (3), 797–815.
- (2) Young, W.-S.; Kuan, W.-F.; Epps, T. H. Block Copolymer Electrolytes for Rechargeable Lithium Batteries. *J. Polym. Sci. Part B Polym. Phys.* **2014**, *52* (1), 1–16.
- (3) Zhang, Z.; Shao, Y.; Lotsch, B. V.; Hu, Y.-S.; Li, H.; Janek, J.; Nan, C.; Nazar, L.; Maier, J.; Armand, M.; et al. New Horizons for Inorganic Solid State Ion Conductors. *Energy Environ. Sci.* **2018**, *11*, 1945–1976.
- (4) Kamaya, N.; Homma, K.; Yamakawa, Y.; Hirayama, M.; Kanno, R.; Yonemura, M.; Kamiyama, T.; Kato, Y.; Hama, S.; Kawamoto, K.; et al. A Lithium Superionic Conductor. *Nat. Mater.* **2011**, *10* (9), 682–686.
- (5) Kato, Y.; Hori, S.; Saito, T.; Suzuki, K.; Hirayama, M.; Mitsui, A.; Yonemura, M.; Iba, H.; Kanno, R. High-Power All-Solid-State Batteries Using Sulfide Superionic Conductors. *Nat. Energy* **2016**, *1* (4), 16030.
- (6) Berthier, C.; Gorecki, W.; Minier, M.; Armand, M. B.; Chabagno, J. M.; Rigaud, P. Microscopic Investigation of Ionic Conductivity in Alkali Metal Salts-Poly(Ethylene Oxide) Adducts. *Solid State Ionics* **1983**, *11* (1), 91–95.

- (7) Gaines, T. W.; Schulz, M. D.; Trigg, E. B.; Winey, K. I.; Wagener, K. B. Precision Sulfonic Acid Polyolefins via Heterogenous to Homogenous Deprotection. *Macromol. Chem. Phys.* **2018**, *219*, 1700634.
- (8) Trigg, E. B.; Gaines, T. W.; Maréchal, M.; Moed, D. E.; Rannou, P.; Wagener, K. B.; Stevens, M. J.; Winey, K. I. Self-Assembled Highly Ordered Acid Layers in Precisely Sulfonated Polyethylene Produce Efficient Proton Transport. *Nat. Mater.* **2018**, *17*, 725–731.
- (9) Cheng, S.; Smith, D. M.; Li, C. Y. How Does Nanoscale Crystalline Structure Affect Ion Transport in Solid Polymer Electrolytes? *Macromolecules* **2014**, *47* (12), 3978–3986.
- (10) Sato, T.; Hayasaka, Y.; Mitsuishi, M.; Miyashita, T.; Nagano, S.; Matsui, J. High Proton Conductivity in the Molecular Interlayer of a Polymer Nanosheet Multilayer Film. *Langmuir* **2015**, *31* (18), 5174–5180.
- (11) Matsui, J.; Miyata, H.; Hanaoka, Y.; Miyashita, T. Layered Ultrathin Proton Conductive Film Based on Polymer Nanosheet Assembly. *ACS Appl. Mater. Interfaces* **2011**, *3* (5), 1394–1397.
- (12) Cheng, S.; Smith, D. M.; Pan, Q.; Wang, S.; Li, C. Y. Anisotropic Ion Transport in Nanostructured Solid Polymer Electrolytes. *RSC Adv.* **2015**, *5* (60), 48793–48810.
- (13) Hayasaka, Y.; Matsui, J.; Miyashita, T. Layered Ultrathin Ion Conductive Membrane Using Polymer Nanosheet with Amine Group. *Mol. Cryst. Liq. Cryst.* **2013**, *579* (1), 17–21.
- (14) Sato, T.; Tsukamoto, M.; Yamamoto, S.; Mitsuishi, M.; Miyashita, T.; Nagano, S.; Matsui, J. Acid-Group-Content-Dependent Proton Conductivity Mechanisms at the Interlayer of Poly(N-Dodecylacrylamide-Co-Acrylic Acid) Copolymer Multilayer Nanosheet Films. *Langmuir* **2017**, *33* (45), 12897–12902.
- (15) Rembaum, A.; Baumgartner, W.; Eisenberg, A. Aliphatic Ionenenes. *Polym. Lett.* **1968**, *6*, 159–171.
- (16) Kunitake, T.; Nakashima, N.; Takarabe, K.; Nagai, M.; Tsuge, A.; Yanagi, H. Vesicles of Polymeric Bilayer and Monolayer Membranes. *J. Am. Chem. Soc.* **1981**, *28* (5), 5945–5947.
- (17) Kunitake, T.; Tsuge, A.; Takarabe, K. Formation of Molecular Membranes in Water from Ionene Oligomes and Related Amphiphiles. *Polym. J.* **1985**, *17* (4), 633–640.

- (18) de Ten Hove, C. L. F.; Penelle, J.; Ivanov, D. A.; Jonas, A. M. Encoding Crystal Microstructure and Chain Folding in the Chemical Structure of Synthetic Polymers. *Nat. Mater.* **2004**, *3* (1), 33–37.
- (19) Chanda, S.; Ramakrishnan, S. Controlling Interlamellar Spacing in Periodically Grafted Amphiphilic Copolymers. *Macromolecules* **2016**, *49* (9), 3254–3263.
- (20) Hong, J.-D.; Jung, B.-D.; Kim, C. H.; Kim, K. Effects of Spacer Chain Lengths on Layered Nanostructures Assembled with Main-Chain Azobenzene Ionenics and Polyelectrolytes. *Macromolecules* **2000**, *33*, 7905–7911.
- (21) Hosoda, S.; Nozue, Y.; Kawashima, Y.; Utsumi, S.; Nagamatsu, T.; Wagener, K.; Berda, E. B.; Rojas, G.; Baughman, T. W.; Leonard, J. K. Perfectly Controlled Lamella Thickness and Thickness Distribution: A Morphological Study on ADMET Polyolefins. *Macromol. Symp.* **2009**, *282* (1), 50–64.
- (22) Caire da Silva, L.; Rojas, G.; Schulz, M. D.; Wagener, K. B. Acyclic Diene Metathesis Polymerization: History, Methods and Applications. *Prog. Polym. Sci.* **2017**, *69*, 79–107.
- (23) Watson, M.; Wagener, K. B. Functionalized Polyethylene via Acyclic Diene Metathesis Polymerization: Effect of Precise Placement of Functional Groups. *Macromolecules* **2000**, *33* (24), 8963–8970.
- (24) Santonja-Blasco, L.; Zhang, X.; Alamo, R. G. Crystallization of Precision Ethylene Copolymers. In *Polymer Crystallization I: From Chain Microstructure to Processing*; Auriemma, F., Ed.; Springer International Publishing, 2015; pp 133–182.
- (25) Rojas, G.; Inci, B.; Wei, Y.; Wagener, K. B. Precision Polyethylene: Changes in Morphology as a Function of Alkyl Branch Size. *J. Am. Chem. Soc.* **2009**, *131* (47), 17376–17386.
- (26) Boz, E.; Wagener, K. B.; Ghosal, A.; Fu, R.; Alamo, R. G. Synthesis and Crystallization of Precision ADMET Polyolefins Containing Halogens. *Macromolecules* **2006**, *39* (13), 4437–4447.
- (27) Baughman, T. W.; Chan, C. D.; Winey, K.; Wagener, K. B. Synthesis and Morphology of Well-Defined Poly (Ethylene-Co-Acrylic Acid) Copolymers. *Macromolecules* **2007**, *40* (18), 6564–

- 6571.
- (28) Opper, K. L.; Markova, D.; Klapper, M.; Müllen, K.; Wagener, K. B. Precision Phosphonic Acid Functionalized Polyolefin Architectures. *Macromolecules* **2010**, *43* (8), 3690–3698.
- (29) Gaines, T. W.; Trigg, E. B.; Winey, K. I.; Wagener, K. B. High Melting Precision Sulfone Polyethylenes Synthesized by ADMET Chemistry. *Macromol. Chem. Phys.* **2016**, *217* (21), 2351–2359.
- (30) Gaines, T. W.; Nakano, T.; Chujo, Y.; Trigg, E. B.; Winey, K. I.; Wagener, K. B. Precise Sulfite Functionalization of Polyolefins via ADMET Polymerization. *ACS Macro Lett.* **2015**, *4* (6), 624–627.
- (31) Berda, E. B.; Wagener, K. B. Probing the Effects of Hydrophilic Branch Size, Distribution, and Connectivity in Amphiphilic Polyethylene. *Macromol. Chem. Phys.* **2008**, *209* (15), 1601–1611.
- (32) Berda, E. B.; Lande, R. E.; Wagener, K. B. Precisely Defined Amphiphilic Graft Copolymers. *Macromolecules* **2007**, *40* (24), 8547–8552.
- (33) Roy, R. K.; Gowd, E. B.; Ramakrishnan, S. Periodically Grafted Amphiphilic Copolymers: Nonionic Analogues of Ionenenes. *Macromolecules* **2012**, *45* (7), 3063–3069.
- (34) Mandal, J.; Ramakrishnan, S. Periodically Grafted Amphiphilic Copolymers: Effects of Steric Crowding and Reversal of Amphiphilicity. *Langmuir* **2015**, *31* (22), 6035–6044.
- (35) Mandal, J.; Krishna Prasad, S.; Rao, D. S. S.; Ramakrishnan, S. Periodically Clickable Polyesters: Study of Intrachain Self-Segregation Induced Folding, Crystallization, and Mesophase Formation. *J. Am. Chem. Soc.* **2014**, *136* (6), 2538–2545.
- (36) Aitken, B. S.; Buitrago, C. F.; Heffley, J. D.; Lee, M.; Gibson, H. W.; Winey, K. I.; Wagener, K. B. Precision Ionomers: Synthesis and Thermal/Mechanical Characterization. *Macromolecules* **2012**, *45* (2), 681–687.
- (37) Trigg, E. B.; Stevens, M. J.; Winey, K. I. Chain Folding Produces a Multilayered Morphology in a Precise Polymer: Simulations and Experiments. *J. Am. Chem. Soc.* **2017**, *139* (10), 3747–3755.
- (38) Trigg, E. B.; Middleton, L. R.; Moed, D. E.; Winey, K. I. Transverse Orientation of Acid Layers in

- the Crystallites of a Precise Polymer. *Macromolecules* **2017**, *50* (22), 8988–8995.
- (39) Ortmann, P.; Trzaskowski, J.; Krumova, M.; Mecking, S. Precise Microstructure Self-Stabilized Polymer Nanocrystals. *ACS Macro Lett.* **2013**, *2* (2), 125–127.
- (40) Yan, L.; Bustillo, K. C.; Panova, O.; Minor, A. M.; Winey, K. I. Solution-Grown Crystals of Precise Acid- and Ion-Containing Polyethylenes. *Polymer* **2018**, *135*, 111–119.
- (41) Buitrago, C. F.; Jenkins, J. E.; Opper, K. L.; Aitken, B. S.; Wagener, K. B.; Alam, T. M.; Winey, K. I. Room Temperature Morphologies of Precise Acid- and Ion-Containing Polyethylenes. *Macromolecules* **2013**, *46* (22), 9003–9012.
- (42) Trigg, E. B.; Middleton, L. R.; Yan, L.; Winey, K. I. Comparing Morphological Evolution during Tensile Deformation of Two Precise Polyethylenes via 2D Fitting of *in Situ* X-Ray Scattering. *Macromolecules* **2018**, *51*, acs.macromol.8b01639.
- (43) Trigg, E. B.; Stevens, M. J.; Winey, K. I. Chain Folding Produces a Multilayered Morphology in a Precise Polymer: Simulations and Experiments. *J. Am. Chem. Soc.* **2017**, *139* (10), 3747–3755.
- (44) Schmidt, R.; Griesbaum, K.; Behr, A.; Biedenkapp, D.; Voges, H.-W.; Garbe, D.; Paetz, C.; Collin, G.; Mayer, D.; Hoke, H. Hydrocarbons. In *Ullmann's Encyclopedia of Industrial Chemistry*; 2000; pp 1–74.
- (45) Lewis, R. N.; McElhaney, R. N. Calorimetric and Spectroscopic Studies of the Polymorphic Phase Behavior of a Homologous Series of N-Saturated 1,2-Diacyl Phosphatidylethanolamines. *Biophys. J.* **1993**, *64* (4), 1081–1096.
- (46) Seddon, J. M.; Cevc, G.; Kaye, R. D.; Marsh, D. X-Ray Diffraction Study of the Polymorphism of Hydrated Diacyl- and Dialkylphosphatidylethanolamines. *Biochemistry* **1984**, *23* (12), 2634–2644.
- (47) Choi, U. H.; Middleton, L. R.; Soccio, M.; Buitrago, C. F.; Aitken, B. S.; Masser, H.; Wagener, K. B.; Winey, K. I.; Runt, J. Dynamics of Precise Ethylene Ionomers Containing Ionic Liquid Functionality. *Macromolecules* **2015**, *48*, 410–420.
- (48) German, I.; Dagosto, F.; Boisson, C.; Tencé-Girault, S.; Soulié-Ziakovic, C. Microphase Separation and Crystallization in H-Bonding End-Functionalized Polyethylenes. *Macromolecules*

- 2015**, *48* (10), 3257–3268.
- (49) Lacombe, J.; Pearson, S.; Pirolet, F.; Norsic, S.; D'Agosto, F.; Boisson, C.; Soulié-Ziakovic, C. Structural and Mechanical Properties of Supramolecular Polyethylenes. *Macromolecules* **2018**, *51* (7), 2630–2640.
- (50) Lacombe, J.; Soulié-Ziakovic, C. Lamellar Mesoscopic Organization of Supramolecular Polymers: A Necessary Pre-Ordering Secondary Structure. *Polym. Chem.* **2017**, *8* (38), 5954–5961.
- (51) Trigg, E. B.; Tiegs, B. J.; Coates, G. W.; Winey, K. I. High Morphological Order in a Nearly Precise Acid-Containing Polymer and Ionomer. *ACS Macro Lett.* **2017**, *6* (9), 947–951.
- (52) Lieser, G.; Wegner, G.; Wagener, K. B.; Smith, J. a. Morphology and Packing Behavior of Model Ethylene/Propylene Copolymers with Precise Methyl Branch Placement. *Colloid Polym. Sci.* **2004**, *282* (8), 773–781.
- (53) Tasaki, M.; Yamamoto, H.; Hanesaka, M.; Tashiro, K.; Boz, E.; Wagener, K. B.; Ruiz-Orta, C.; Alamo, R. G. Polymorphism and Phase Transitions of Precisely Halogen-Substituted Polyethylene. (1) Crystal Structures of Various Crystalline Modifications of Bromine-Substituted Polyethylene on Every 21st Backbone Carbon. *Macromolecules* **2014**, *47* (14), 4738–4749.
- (54) Buitrago, C. F.; Opper, K. L.; Wagener, K. B.; Winey, K. I. Precise Acid Copolymer Exhibits a Face-Centered Cubic Structure. *ACS Macro Lett.* **2012**, *1* (1), 71–74.
- (55) Zhao, Y. H.; Abraham, M. H.; Zissimos, A. M. Fast Calculation of van Der Waals Volume as a Sum of Atomic and Bond Contributions and Its Application to Drug Compounds. *J. Org. Chem.* **2003**, *68* (19), 7368–7373.
- (56) Blanco, F. J.; Rivas, G.; Serrano, L. A Short Linear Peptide That Folds into a Native Stable  $\beta$ -Hairpin in Aqueous Solution. *Nat. Struct. Biol.* **1994**, *1* (9), 584–590.
- (57) Kretsinger, J. K.; Haines, L. A.; Ozbas, B.; Pochan, D. J.; Schneider, J. P. Cytocompatibility of Self-Assembled  $\beta$ -Hairpin Peptide Hydrogel Surfaces. *Biomaterials* **2005**, *26* (25), 5177–5186.

## Table of Contents

Precisely periodic functional groups induce controlled hairpin folding in some polymers, forming ordered sub-nanometer layers that promote ion transport.

